A R C H I V E O F M E C H A N I C A L E N G I N E E R I N G

VOL. LXI 2014 Number 2

10.2478/meceng-2014-0015

Key words: multibody dynamics, nonsmooth dynamics, contact, timestepping methods, co-simulation

MATTEO FANCELLO [*], *MARCO MORANDINI* [*], *PIERANGELO MASARATI* [*]

HELICOPTER ROTOR SAILING BY NON-SMOOTH DYNAMICS CO-SIMULATION

This paper presents the application of a co-simulation approach for the simulation of frictional contact in general-purpose multibody dynamics to a rotorcraft dynamics problem. The proposed approach is based on the co-simulation of a main problem, which is described and solved as a set of differential algebraic equations, with a subproblem that is characterized by nonsmooth dynamics events and solved using a timestepping technique. The implementation and validation of the formulation is presented. The method is applied to the analysis of the droop and anti-flap contacts of helicopter rotor blades. Simulations focusing on the problem of blade sailing are conducted to understand the behavior and assess the validity of the method. For this purpose, the results obtained using a contact model based on Hertzian reaction forces at the interface are compared with those of the proposed approach.

1. Introduction

In mechanics, the problem of unilateral constraints, like frictionless and frictional contact phenomena in multi-rigid-body problems, is characterized by nonsmooth dynamics. Broadly speaking, the problem can be dealt with following two approaches: using continuous contact, in an attempt to exploit smooth dynamics, or using hard constraints, with complementarity approaches. In the first case the nonsmooth aspects of the problem are regularized, for example by replacing the non-interpenetration constraint at contact with a very stiff spring that is activated when collision is detected [1, 2]. Conversely, the complementarity approach is built on the basis of a mathematical framework able to consistently describe solutions that include nonsmooth-

[*] *Politecnico di Milano, Dipartimento di Scienze e Tecnologie Aerospaziali, via La Masa 34, 20156 Milano - Italy; E-mail: matteo.fancello@gmail.com, marco.morandini@polimi.it, pierangelo.masarati@polimi.it*

ness, through the description of the phenomena in terms of Complementarity Problems (CP) [2, 4, 5].

This work originates from an exploratory attempt of integrating the capability to consistently model unilateral constraints in a general purpose multibody formulation and implementation originally designed to address intrinsically smooth problems, MBDyn[1]. This free general purpose multibody dynamics analysis software, released under GNU Public License (GPL) 2.1[2] has been developed at the Department of Aerospace Science and Technology of the University "Politecnico di Milano", Italy [6]. Among state of the art complementarity problem approaches, the classic Moreau-Jean timestepping [4] has been considered to implement frictionless and frictional contacts through a co-simulation approach in the general purpose solver [7, 8].

The focus is on generally smooth problems, characterized by significant multidisciplinarity, with the need to selectively include non-smooth events localized in time and in specific components of the model. For this reason, rather than redesigning from scratch a monolithic nonsmooth solver capable of handling all the required types of problems, a co-simulation approach is devised between the smooth multidisciplinary solver and the Non-Smooth Contact Dynamics (NSCD) framework, with the use of components from Siconos, a library developed and distributed by INRIA[3]. Co-simulation with existing state-of-art nonsmooth timestepping solvers is expected to provide a satisfactory solution that does not require to "reinvent the wheel" in solvers specifically designed for smooth problems, like MBDyn, by reformulating the whole problem in the nonsmooth framework. Indeed, important efforts like Saladyn[4] and Chrono[5] already point in this second direction.

The problem is solved by co-simulating a nonsmooth subset of the problem, using timestepping methods with a velocity-impulse formulation based on a Linear Complementarity Problem (LCP), along with the mainly smooth part, formulated as Differential-Algebraic Equations (DAEs), using A/L stable multistep algorithms.

2. Implementation and Validation Aspects

The nonsmooth subproblem is confined in a portion of the model where nonsmooth events are expected to occur. The nonsmooth subproblem accounts for the dynamics of a point mass and its contact with interacting

[1] `http://www.mbdyn.org/`, last accessed November 2013
[2] `http://www.gnu.org/licenses/licenses.html`, last accessed November 2013
[3] `http://siconos.gforge.inria.fr/`, last accessed November 2013
[4] `http://saladyn.gforge.inria.fr/`, last accessed November 2013
[5] `http://www.chronoengine.info/`, last accessed November 2013

surfaces. The nonsmooth point mass interacts with the smooth portion of the problem by means of a coincidence kinematic constraint that is enforced between the kinematics of the nonsmooth point and that of an interface node of the smooth domain. The enforcement of the coincidence constraint in the smooth problem formulation produces reaction forces, described by the Lagrange multipliers associated with the coincidence constraint, that are applied to the point mass in the nonsmooth problem as external forces. Multiple independent instances of the nonsmooth subproblem may be defined.

From an implementation point of view, the nonsmooth subproblem is confined in a user-defined element implemented as a run-time loadable module, the nonsmooth-node module, without requiring any modification to MBDyn's core code. In order to have a versatile tool to model contact points, the nonsmooth subsystem is represented by a single node possibly subjected to contact with one or more planes.

The interface between the smooth and the nonsmooth domains consists in enforcing compatibility between this node integrated with timestepping and an interface node from the MBDyn model. The smooth part of the problem receives prescribed displacement and velocity at the interface, which are imposed using kinematic constraints with Lagrange multipliers. The reaction forces are passed back to the nonsmooth solver. The two solutions are iterated until mutual convergence is reached at each time step.

The dynamics of the contact subsystem is described by the measure differential equation,

$$\mathbf{M}\mathrm{d}\dot{\mathbf{q}} = \mathbf{f}(\mathbf{q}, \dot{\mathbf{q}}, t)\mathrm{d}t + \mathrm{d}\mathbf{r}, \tag{1}$$

where $\mathrm{d}t$ is the Lebesgue measure, $\mathrm{d}\dot{\mathbf{q}}$ is a differential measure representing the acceleration measure, $\mathrm{d}\mathbf{r}$ is a non-negative real measure representing the reaction forces and impulses, and $\mathbf{f}$ includes the forces acting on the node of the multi-body main model associated with the contact node, and by a unilateral constraint,

$$0 \leqslant U^{(+)} + e \cdot U^{(-)} \perp \Lambda \geqslant 0 \tag{2}$$

The unilateral constraint, associated with a Newton restitution law, is formulated in Eq. (2) as a complementary condition between gap velocity U and impulse Λ [3].

The dynamics of this subsystem is integrated with the NSCD method, an event-capturing approach for multi-rigid-body dynamics initiated and developed by J. J. Moreau and M. Jean [3, 4]. This first order timestepping method advances each step by discretizing Eqs. (1) and (2) in time and formulating a linear complementarity problem in the unknowns U_{k+1} and Λ_{k+1}, the generalized velocity at the end of the time step and the impulse.

The CP is solved by a Lemke algorithm [9], through the use of the library Siconos Numerics, and the values of the generalized position and velocity for the current iteration are updated.

Time is discretized on intervals $(t_n, t_{n+1}]$ of length h using the Moreau mid-point scheme,

$$\mathbf{M}(\mathbf{v}_{n+1} - \mathbf{v}_n) = h\theta\mathbf{f}_{n+1} + h(1-\theta)\mathbf{f}_n + \mathbf{r}_{n+1} \tag{3a}$$

$$\mathbf{q}_{n+1} = \mathbf{q}_n + h\theta\mathbf{v}_{n+1} + h(1-\theta)\mathbf{v}_n, \tag{3b}$$

with $\theta = 1/2$, where $\mathbf{v}_{n+1}$ represents the approximation of the right limit of velocity at time t_{n+1}, i.e. $\dot{\mathbf{q}}^+_{n+1}$. Eq. (3a) can be written as

$$\mathbf{v}_{n+1} = \mathbf{v}_{n,\text{free}} + \mathbf{M}^{-1}\mathbf{r}_{n+1}, \tag{4}$$

where $\mathbf{v}_{\text{free}}$ is a vector that collects the terms representing the velocity of the system when reaction forces are null. A contact law of the kind of Eq. (2) must be added to Eq. (4), so that the basic contact problem that must be solved to advance the step can be expressed in the local reference frame as

$$\mathbf{u}_{n+1} = \mathbf{W}\mathbf{r}_{n+1} + \mathbf{u}_{\text{free}}, \tag{5}$$

where $\mathbf{W} = \mathbf{H}^T\mathbf{M}^{-1}\mathbf{H}$ is the Delassus operator, which models the local behavior of the solids at the contact point.

At each step, the algorithm forms an index of the closed constraints using a rough prediction of the state, and assembles the LCP that must be solved to advance time by one step. The state is subsequently updated using Eq. (3b).

A comprehensive and clear presentation of the NSCD method, with details about the assembly of the LCP in presence of multiple constraints, is included in [5].

The proposed co-simulation approach has been validated and its properties evaluated empirically by comparison with results from entirely nonsmooth methods for simple applications of academic interest, as detailed in [8]. Three benchmarks, the classic ball falling on a plane, the linear oscillator and a chain of masses encountering a unilateral constraint have been considered, and results from the co-simulation approach have been compared with results from classic Moreau-Jean timestepping, from a nonsmooth adaptation of the Hilbert-Hughes-Taylor (HHT) integration scheme [10] and of an original multistep formula [11, 6]. Figure 1 shows results for one of the three models considered.

The approach has also been applied to frictional contact problems by extending the formulation of the nonsmooth problem with a polyhedral approximation of Coulomb's cone [12]. Such extension is not detailed here because it is not relevant for the rotor sailing problem. The validation of the approach and its application to a walking mechanism are presented in [8].

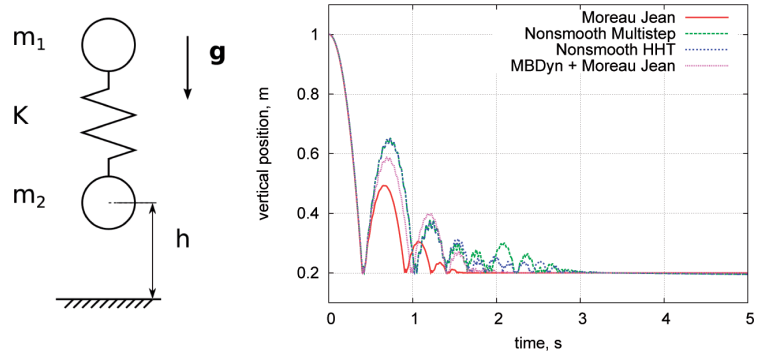

(a) Model (b) Vertical position comparison

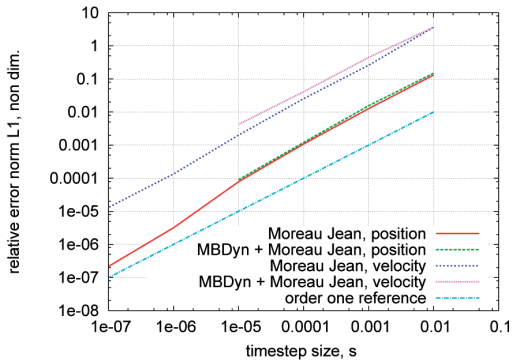

(c) Error in L1 norm

Fig. 1. Linear oscillator example

3. Helicopter Rotor Flap-Stop Contact Analysis

The coupled solver described in previous sections is applied to the analysis of rotor sailing, a complex intermittent contact problem in rotorcraft dynamics.

The design of an articulated rotor needs to include support points in correspondence of the blade cuff to overcome the effect of the blade weight at low rotation speeds. These contact devices are called droop stops. Moreover, during start-up and shutdown operations, rotorcraft blades are spinning at low velocity and therefore can be subjected to high wind-induced aerodynamic forces without the benefit of the centrifugal stiffening present at operating angular velocities. An additional restraint is thus required to prevent the upward vertical motion of the blade. The anti-flap assembly provides such restraint.

In such conditions the aeroelastic phenomenon of blade sailing can cause a potentially dangerous blade motion and generate excessive flapwise tip de-

flections [13]. This phenomenon is particularly relevant for naval helicopters, where high winds, also in combination with interference and vorticity caused by the ship structure, and motion induced by ship roll and pitch, can cause severe damage to the airframe, the flight crew and the flight deck personnel.

In the literature, considerable attention has been paid to the problem of blade sailing and to the development of analysis tools suitable to simulate it [14, 15, 16, 17]. Geyer et al. [14] present an analysis of shipborne rotor sailing where an original rotor aeroelastic model based on 2D aerodynamics and finite element structural dynamics is subjected to the dynamic and aerodynamic effects of ship motion. Bottasso and Bauchau [15] formulated the problem within the framework of finite element based flexible multibody dynamics. In [15] the unilateral contact condition is enforced as a nonlinear holonomic constraint via the Lagrange multiplier technique. Kang and He [16] used commercial software to develop a multibody formulation of a helicopter and ship, including realistic ship motion and contributions from the helicopter suspension to the dynamics of the problem. In [17] Wall et al. address the efficient modeling and validation of the ship-helicopter-rotor system with rigid-body and flexible-element dynamics. Here the droop and flap stops are modeled by an added hinge stiffness in correspondence to the stop contact angles.

3.1. Modeling Approaches

The devised co-simulation with a nonsmooth contact subsystem is included here in a finite element based multibody dynamics formulation providing an analysis tool to model the droop-stop and anti-flap stop contact mechanism of helicopter rotors in different operating conditions.

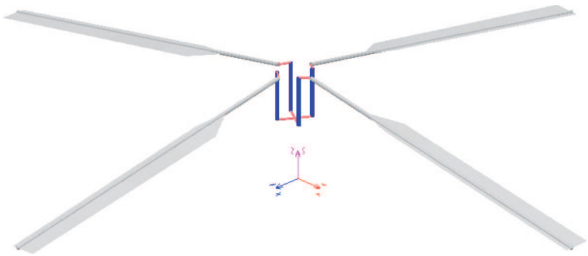

Fig. 2. Aeroelastic model of the SA330 Puma articulated rotor

A nonlinear multibody aeroelastic model of the SA330 Puma helicopter, implemented in MBDyn and shown in Fig. 2, has been analyzed. The model was developed in previous works (see for example [18, 19]) using the appendix of [20] as the main source of data.

The main rotor is modeled using the multibody approach. Kinematically exact constraints, enforced by means of Lagrange multipliers, describe the relative motion between rigid bodies; structural dynamics are dealt with by a finite element-like approach using nonlinear, geometrically exact beam elements based on an original formulation [21], whereas inertia is accounted for by lumping masses at the nodes. Built-in blade-element (2D) aerodynamics with a simple inflow model based on momentum theory are used.

In the present analysis the main rotor hub is constrained to the ground by a joint that prescribes the angular velocity. Each blade is hinged to the rotor hub by a sequence of revolute joints that connect rigid bodies, describing, from the hub towards the blade tip, the lead-lag and the flap hinges, and the pitch bearing. From the pitch bearing on, each blade is modeled using 5 three-node beam elements. The innermost structural node that belongs to the flexible portion of the blade and is connected to the pitch bearing is also connected to the rigid body that describes the rotating portion of the swashplate by a flexible rod element, thus realistically introducing blade pitch control in a manner that is kinematically exact and dynamically consistent with the finite element approximation. The geometric, structural and aerodynamic properties of the problem have been extracted from [20].

Two ways of describing the contact at droop-stops and anti-flap stops have been implemented: the proposed co-simulation approach and a continuous contact modelization.

3.1.1. Nonsmooth Dynamics Approach

In the first case, the differential-algebraic model of the rotor has been associated with a co-simulated subsystem comprising each blade's node that is responsible for contact with the flap stop surfaces. The mechanism is described as a contact point rigidly attached under the first node after the flap hinge, with an offset. Such node, representing the contact point, has its motion limited by two vertical planes. The planes define the limit angles that the blade root can assume with respect to the horizontal plane when flapping (± 10 deg). The nodes subjected to the unilateral constraint represent the nonsmooth subsystems that are integrated by the co-simulation module. The unilateral constraints are defined as planes rigidly attached to the rotor hub, and thus rotate with it when the rotor is spun. The geometry of the contact model is detailed in Fig. 3. In the figure, one of the planes that model the unilateral constraint is visualized, and the point of contact is highlighted as a small (red) ball.

The contact node is linked to the blade cuff through a rigid joint constraining its offset position and orientation in relation with the first node

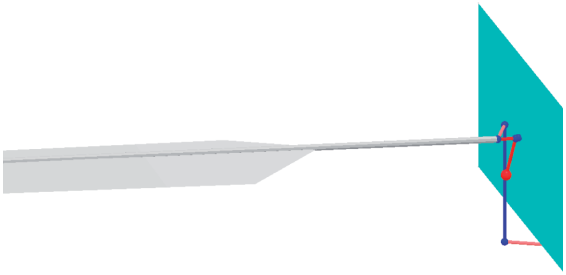

Fig. 3. Contact modeled as a nonsmooth subsystem comprising a node (the red ball) impacting a plane

after the flap hinge, at the root of the blade. The contact constraint formally closes a kinematic chain between the rotor hub and the flapping part of the blade, since it prescribes the coincidence of the contact node with the flapping part of the blade, and at the same time that of the contact plane with the hub. As a consequence, the problem becomes overconstrained, and the Jacobian matrix becomes singular. To compensate for the overconstraining, the coincidence joint must be relaxed. Such relaxation has been implemented using the "Tikhonov" regularization element, which is currently available in the element library of MBDyn, and is described in the following. Given the index 3 DAE problem

$$\boldsymbol{f}\left(\mathbf{q}, \dot{\mathbf{q}}, \ddot{\mathbf{q}}, t\right) + \boldsymbol{\Phi}_{/\mathbf{q}}^{T} \boldsymbol{\lambda} = 0 \tag{6a}$$

$$\boldsymbol{\Phi}\left(\mathbf{q}\right) = 0, \tag{6b}$$

the Tikhonov regularization allows the violation of the constraint equation $\boldsymbol{\Phi}(\mathbf{q}) = \mathbf{0}$ by an amount that is proportional to the corresponding multiplier $\boldsymbol{\lambda}$,

$$\boldsymbol{f}\left(\mathbf{q}, \dot{\mathbf{q}}, \ddot{\mathbf{q}}, t\right) + \boldsymbol{\Phi}_{/\mathbf{q}}^{T} \boldsymbol{\lambda} = 0 \tag{7a}$$

$$\boldsymbol{\Phi}\left(\mathbf{q}\right) - c\boldsymbol{\lambda} = 0 \tag{7b}$$

where c is a user-defined constant that represents a compliance. The larger the coefficient c is, the larger the constraint violation can be for a given value of the multiplier $\boldsymbol{\lambda}$. The index of the DAE problem reduces from 3 of Eqs. (6) to 1 of Eqs. (7). This formulation resembles the so-called Augmented Lagrangian[6] (AL) approach discussed by García de Jalón and Bayo [22], and attributed to Bayo et al. [23]. The AL can be obtained by computing $\boldsymbol{\lambda}$ from Eq. (7b) and substituting it in Eq. (7a). In the present formulation, Eqs. (7), the equations and unknown variables layout of Eqs. (6) is preserved.

[6] The original formulation of [23] actually used a linear combination of the constraint equation and its first- and second-order derivatives, thus expressing the constraint reactions as functions of the constraint violation and its time derivatives.

This specific application highlights the versatility of the co-simulation module implementation, which makes it possible to add points of frictionless and frictional contact to a model in which the nonsmoothness due to the unilaterality of the constraints is dealt with using event-capturing timestepping techniques that cope well with the implicit integration approach of the original smooth problem solution. However, this application is also particularly challenging for the concept, since through the rigid joint the co-simulated subsystems are very tightly coupled, requiring a small time step for successful and rapid convergence of the co-simulation.

3.1.2. Continuous Contact Approach

A second approach for the contact has been implemented to compare and validate the results. In this latter case the problem is purely differential-algebraic, the non-smooth event being regularized using a penalty-like approach. The unilateral constraint has been modeled as a "revolute" joint with a stiff "continuous contact" reaction law activated at prescribed constraint angles. This modelization is similar to the approach adopted in [17], where the choice of added stiffness to model the hinge backlash is here replaced with a reaction law that more accurately describes the physical interaction. It is worth noticing that also the "continuous contact" constitutive law was implemented as a run-time loadable module and used by existing 1D connectivity elements (e.g. rods and deformable axial joints).

The visco-elastic Hertzian formulation shown in Eq. (8), describing the force-deformation relationship for the contacting bodies proposed by Flores et al. [2], has been implemented. The dissipation term is formulated as a function of the desired Newton restitution coefficient e, as in the original formulation proposed by Hunt and Crossley [1], and the reaction force f is a function of the allowed interpenetration (or "gap") δ,

$$f = K\delta^n \left(1 + \frac{8}{5}\frac{(1-e)}{e}\frac{1}{\dot{\delta}^{(-)}} \cdot \dot{\delta}\right) \tag{8}$$

The term $\dot{\delta}^{(-)}$ in Eq. (8) represents the gap rate when the contact begins. As such, it is always positive; a threshold is considered to account for contacts at extremely slow speed.

A "revolute" joint coincident with the blade flap hinge is provided with two constitutive laws of the kind in Eq. (8) in correspondence of the angles at which the droop and anti-flap mechanisms intervene, which provide a corresponding reaction moment about the "revolute" joint axis. To correctly characterize the elastic behavior of metal to metal contact, the generalized stiffness parameter K in Eq. (8) must be formulated in relation with the

material properties and shape of the contact surfaces [24]. For a steel-to-steel contact this requirement translates into a very high stiffness, as shown in Table 1; such a high stiffness requires a very small time step when the contact is active (i.e. when δ is positive).

3.2. Analyzed Problems

Two operational conditions of interest have been simulated to gain insight into the properties and validity of the contact modelization.

3.2.1. Rotor Engagement and Disengagement

In the first simulation, the rotor engagement and disengagement phases have been considered. The simulation is a bit shorter than realistic start-stop procedures (20 s as opposed to about one minute or more in realistic operations); it is essentially intended to highlight the capability of the co-simulation approach to model the contact constraint of the flap-stop mechanism.

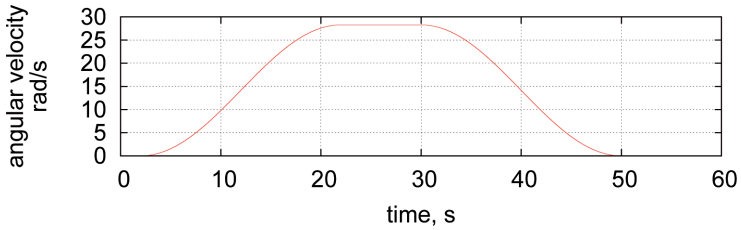

Fig. 4. Rotor start-up and stop simulation: prescribed hub angular velocity profile

The hub rotation speed $\Omega(t)$ throughout the length of the simulation is illustrated in Fig. 4. The velocity reaches the regime value following a cosine law described by Eq. (9),

$$\Omega(t) = \Omega_{100\%} \cdot \left(1 - \cos\left(\frac{\pi}{20} \cdot t\right)\right) \qquad 0 \text{ s} \leq t \leq 20 \text{ s}, \tag{9}$$

and the disengagement phase follows an analogous velocity profile starting at 30 s. The parameter values for the two simulations are presented in Table 1.

The first plot in Fig. 5 illustrates the evolution of the flap and lag angles of blade 1. The motion of the blade throughout the simulation is shown in the top graph. The blades are initially still, their weight supported by the flap stops at an angle of -10 degrees. The initial oscillations of the internal force and moments and of the tip displacement are a consequence of the flexibility of the blade, which is initially unloaded. The initial transient observed in the results is caused by the sudden appearance of gravity loads at the beginning of the simulation. As soon as the rotor winds up, the centrifugal effect moves

Table 1.

Simulation parameters

Nonsmooth Node Model		
Restitution coefficient	0.8	non-dim.
Time step	10^{-4}	s
Tolerance	10^{-4}	non-dim.
Tikhonov constant, c	$5 \cdot 10^{-9}$	rad/(Nm)
Continuous Contact Model		
Constitutive law	Flores et al. [2] ($n = 3/2$)	
Restitution coefficient	0.8	non-dim.
Time step	10^{-4}	s
Tolerance	10^{-4}	non-dim.
Contact stiffness, K	10^9	N/m$^{3/2}$

the blades away from the contact. A constant, nominal angular velocity $\Omega_{100\%}$ is maintained for 10 seconds. Afterwards, the rotor slows down with the same cosine law, but with opposite sign. The centrifugal effect reduces and the blades gently drop down, hitting the droop stops when the flap angle is back to -10 deg. The simulation has been carried out with the collective and cyclic pitch controls set to zero. The properties of the air stream refer to standard air at sea level, still.

The subsequent graphs in Figure 5 present the out-of-plane component of the internal force and the flapwise bending moment in the beam section close to the root of the first blade. The last plot of Fig. 5 shows the blade tip height (the height of the rotor with respect to the origin is about 2.15 m). The results of the continuous contact approach and the modelization through the nonsmooth node are in good agreement. In the initial and end phases of the analysis the vertical shear force peaks are related to the contact with the droop stop. The force and moment oscillate as a consequence of the blade flexibility.

3.2.2. Still Rotor Subjected to Deterministic Gust

To further test the versatility of the model, a different simulation condition has been considered. The rotor, initially still with the four blades resting on the droop stop contacts, is invested by a strong wind gust v_G, whose profile is represented in Fig. 6 (hence the "deterministic" definition, as opposed to "stochastic"). The direction of the uniform gust front and its profile are on the horizontal plane, directed transversely with respect to the first blade:

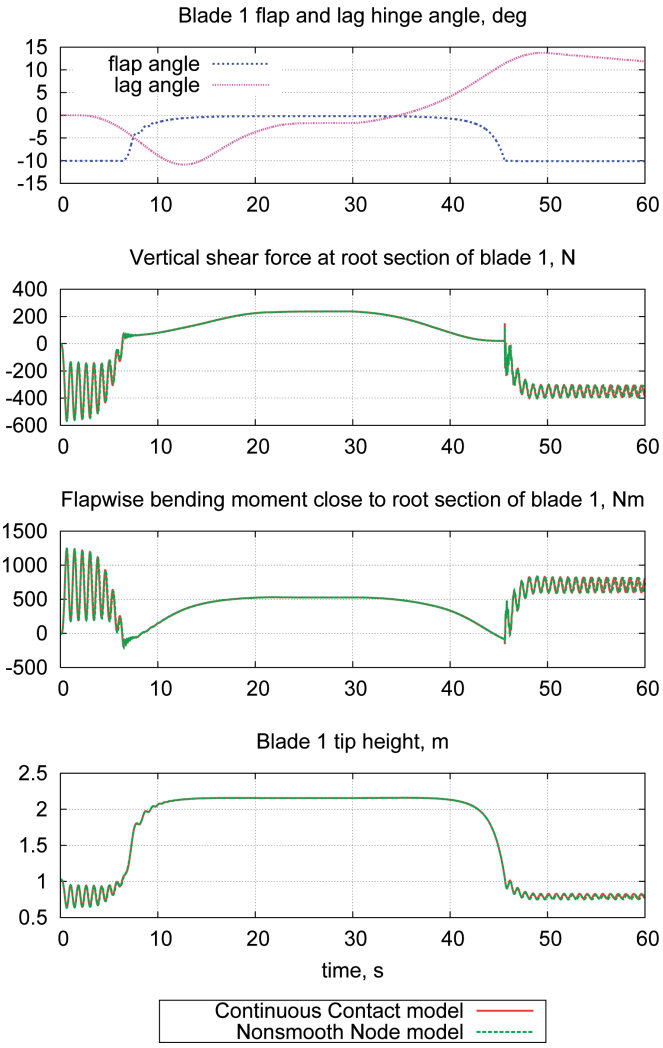

Fig. 5. Rotor wind-up and stop: simulation results

assuming that blade 1 is aligned with global axis x, the gust front travels in time along axis y and the gust velocity $\mathbf{v}_G$ is also directed along axis y, $\mathbf{v}_G = v_G \mathbf{e}_y$. The collective pitch angle for this simulation is 10 degrees. The first blade is raised by the aerodynamic force (remember that the rotor of the SA330 spins clockwise when seen from above), until the flap stop comes into contact. After the gust passes, the blade falls back onto the droop-stop contact, with some bouncing mostly related to the flexibility of the blade. This behavior is illustrated in the first plot of Fig. 7, which shows the flap

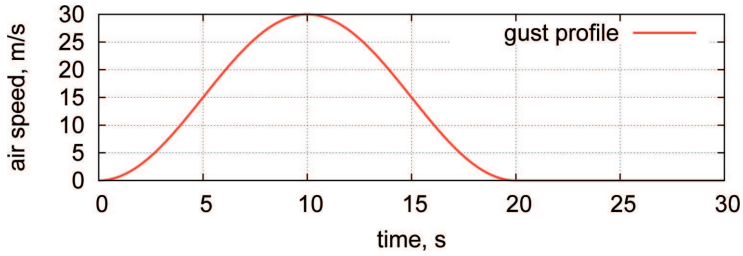

Fig. 6. Gust profile

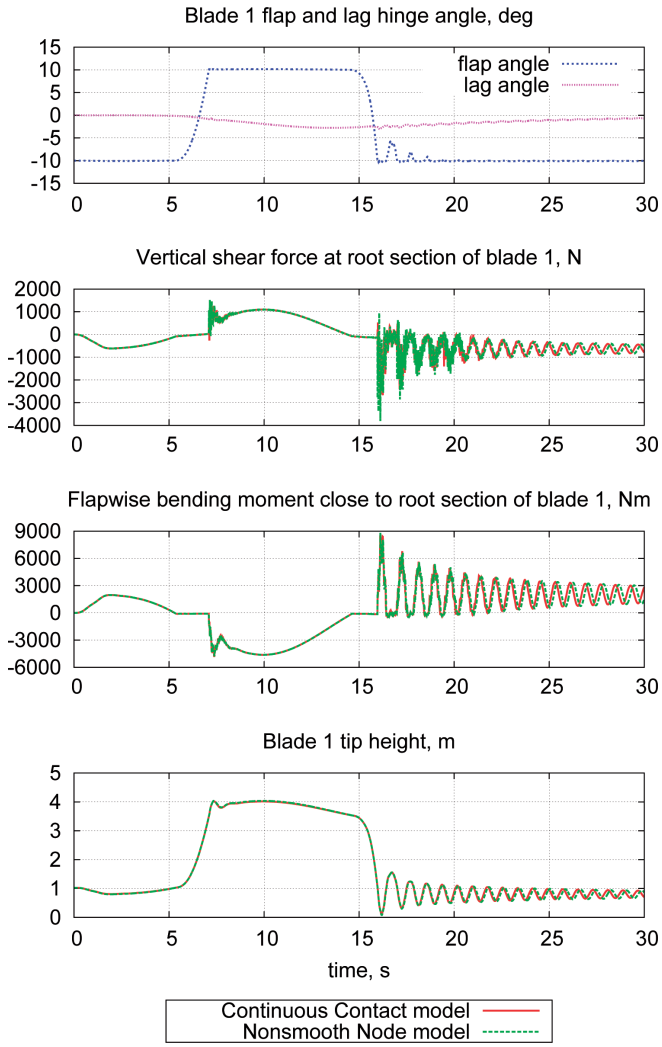

Fig. 7. Gust investing a still rotor: simulation results

and lag hinge angles of the first blade, the former limited by the droop-stop and anti-flap contacts respectively at −10 deg and +10 deg. On the other side of the rotor, the third blade experiences a downward force, and blades 2 and 4 are not sensibly affected by the gust, since the airstream that affects them is essentially radial.

The vertical shear force and the bending moment in the beam section at the root of the first blade are shown in the second and third plot of Fig. 7 for the two models. The last plot of Fig. 7 shows the tip deflection. The results of the continuous contact approach and the modelization through the nonsmooth node correlate well.

4. Conclusions

An approach to contact modeling in multibody formulations by co-simulation with an integrated nonsmooth contact dynamics subsystem is applied in this paper to a complex problem in rotorcraft aeromechanics. The droop and flap stops of a helicopter rotor are modeled using both the devised approach and a continuous contact approach, substituting the unilateral constraint with a steep force-deformation constitutive law activated at contact.

The different solutions for the modeling of the intermittent contact are compared in the simulation of operational conditions that are relevant in the study of aeroelastic phenomena referred to as rotor blade sailing.

The results show the soundness of the proposed co-simulation approach, which can provide a versatile tool to add some frictionless and frictional contact capabilities to multibody formulations without requiring the complete reformulation of the dynamics in a nonsmooth dynamics simulation framework.

Manuscript received by Editorial Board, December 03, 2013;
final version, February 05, 2014.

REFERENCES

[1] Hunt K. H., Crossley F. R. E.: Coefficient of restitution interpreted as damping in vibroimpact. Journal of Applied Mechanics, Transactions ASME, 42(2), 440-445, 1975. doi:10.1115/1.3423596.

[2] Flores P., Machado M., Silva M. T., and Martins J. M.: On the continuous contact force models for soft materials in multibody dynamics. Multibody System Dynamics, 25(3), 357-375, March 2011. doi:10.1007/s11044-010-9237-4.

[3] Moreau J. J.: Unilateral contact and dry friction in finite freedom dynamics. Nonsmooth mechanics and applications, CISM, Courses and lectures, Springer-Verlag, 302, 1-82, 1988.

[4] Jean M.: The nonsmooth contact dynamics method. Comput. Meth. Appl. Mech. Engng., 177(3-4), 235-257, 1999. doi:10.1016/S0045-7825(98)00383-1.

[5] Acary V., and Brogliato B.: Numerical Methods for Nonsmooth Dynamical Systems. Springer, 2008.

[6] Masarati P., Morandini M., and Mantegazza P.: An efficient formulation for general-purpose multibody/multiphysics analysis. J. of Computational and Nonlinear Dynamics, in press. doi:10.1115/1.4025628.

[7] Fancello M., Masarati P., and Morandini M.: Smooth/non-smooth dynamics co-simulation of helicopter rotor sailing. In Multibody 2013, Zagreb, Croatia, July 1-4 2013.

[8] Fancello M., Masarati P., and Morandini M.: Adding non-smooth analysis capabilities to general-purpose multibody dynamics by co-simulation. In Proceedings of ASME IDETC/CIE, Portland, OR, August 4-7 2013. DETC2013-12208.

[9] Lemke C. E.: Bimatrix equilibrium points and mathematical programming. Management Science, 11(7), 681-689, May 1965. doi:10.1287/mnsc.11.7.681.

[10] Chen Q., Acary V., Virlez G., and Brüls O.: A newmark-type integrator for flexible systems considering nonsmooth unilateral constraints. In P. Eberhard and P. Ziegler, editors, 2nd Joint International Conference on Multibody System Dynamics, Stuttgart, Germany, May 29-June 1 2012.

[11] Masarati P., Lanz M., and Mantegazza P.: Multistep integration of ordinary, stiff and differential-algebraic problems for multibody dynamics applications. In XVI Congresso Nazionale AIDAA, pages 71.1-10, Palermo, 24-28 September 2001.

[12] Klarbring A.: A mathematical programming approach to three-dimensional contact problems with friction. Comput. Meth. Appl. Mech. Engng., 58(2), 175-200, 1986. doi:10.1016/0045-7825(86)90095-2.

[13] Newman S.: The phenomenon of helicopter rotor blade sailing. Proc. IMechE, Part G: J. Aerospace Engineering, 213(6), 347-363, 1999. doi:10.1243/0954410991533070.

[14] Geyer William P., Smith Edward C., and Keller Jonathan A.: Aeroelastic analysis of transient blade dynamics during shipboard engage/disengage operations. Journal of Aircraft, 35(3), 445-453, 1998. doi:10.2514/2.2317.

[15] Bottasso C. L., and Bauchau O. A.: Multibody modeling of engage and disengage operations of helicopter rotors. Journal of the American Helicopter Society, 46(4), 290-300, 2001. doi:10.4050/JAHS.46.290.

[16] Kang H., and He C.: Modeling and simulation of rotor engagement and disengagement during shipboard operations. In American Helicopter Society 60th Annual Forum, pages 315-324, Baltimore, MD, June 7-10 2004.

[17] Wall A. S., Afagh F. F., Langlois R. G., and Zan S. J.: Modeling helicopter blade sailing: Dynamic formulation and validation. Journal of Applied Mechanics, 75(6), 061004.1-10, 2008. doi:10.1115/1.2957599.

[18] Quaranta G., Bindolino G., Masarati P., and Mantegazza P.: Toward a computational framework for rotorcraft multi-physics analysis: Adding computational aerodynamics to multibody rotor models. In 30th European Rotorcraft Forum, pages 18.1-14, Marseille, France, 14-16 September 2004.

[19] Muscarello V., Masarati P., and Quaranta G.: Multibody analysis of rotorcraft-pilot coupling. In P. Eberhard and P. Ziegler, editors, 2nd Joint International Conference on Multibody System Dynamics, Stuttgart, Germany, May 29-June 1 2012.

[20] Bousman William G., Young C., Toulmay F., Gilbert Neil E., Strawn Roger C., Miller Judith V., Maier Thomas H., Costes M., and Beaumier P.: A comparison of lifting-line and CFD methods with flight test data from a research Puma helicopter. TM 110421, NASA, October 1996.

[21] Ghiringhelli G. L., Masarati P., and Mantegazza P.: A multi-body implementation of finite volume beams. AIAA Journal, 38(1), 131-138, January 2000. doi:10.2514/2.933.

[22] García de Jalón J., and Bayo E.: Kinematic and Dynamic Simulation of Multibody Systems: the Real Time Challenge. Springer-Verlag, New York, 1994.

[23] Bayo E., García de Jalón J., and Serna M. A.: A modified Lagrangian formulation for the dynamic analysis of constrained mechanical systems. Comput. Meth. Appl. Mech. Engng., 71(2), 183-195, 1988. doi:10.1016/0045-7825(88)90085-0.
[24] Goldsmith W.: Impact, The Theory and Physical Behaviour of Colliding Solids. Edward Arnold Ltd, London, England, 1960.

Kosymulacja niegładkiej dynamiki łopat helikoptera w warunkach żeglugowania

S t r e s z c z e n i e

W artykule przedstawiono problem dynamiki wiropłatu rozwiązany przy zastosowaniu ogólnej metody kosymulacji używanej do symulacji kontaktu ciernego w dynamice układu wieloczłonowego. Proponowane podejście jest oparte na kosymulacji głównego problemu, opisanego i rozwiązanego jako układ algebraicznych równań różniczkowych wspólnie z podproblemem, który jest scharakteryzowany przez zdarzenia niegładkiej dynamiki i rozwiązany techniką kroków czasowych. Zaprezentowano implementację i walidację takiego sformułowania. Metodę zastosowano do analizy zwisu i łopotania łopatek wirnika helikoptera. By zrozumieć działanie metody i ocenić jej przydatność przeprowadzono symulacje dotyczące zachowania wirnika helikoptera w warunkach żeglugi. Dla oceny metody porównano wyniki uzyskane przy użyciu modelu kontaktowego wykorzystującego siły reakcji Hertza z wynikami uzyskanymi w proponowanym podejściu.